

Simultaneous measurement of Young's modulus and Poisson's ratio at microscale with two-modes scanning microdeformation microscopy

Julian Le Rouzic^a Patrick Delobelle^b Bernard Cretin^a Pascal Vairac^a
Fabien Amiot^{b,1}

^a*FEMTO-ST Institute, CNRS-UMR 6174 / UFC / ENSMM / UTBM, 32 avenue de l'Observatoire, F-25030 Besançon, France*

^b*FEMTO-ST Institute, CNRS-UMR 6174 / UFC / ENSMM / UTBM, 24 chemin de l'Épitaphe, F-25030 Besançon, France*

1 Introduction

Constant advances in thin coating technology have led to the development of micro- and nanoscale devices, for which the knowledge of mechanical properties of the involved materials is essential to guarantee the capabilities of these systems. Elastic properties are in particular known to be very dependent on the deposition process conditions. Consequently this requires experimental techniques enabling to measure elastic constants of thin coatings

without being disturbed by the influence of the substrate. This has become possible thanks to acoustic microscopy [1], scanning probe microscopy [2,3] and nanoindentation [4,5]. Considering an isotropic material described by its Young's modulus E and its Poisson's ratio ν , these techniques unfortunately only provide a combination of the elastic parameters. Nanoindentation provides for example the measurement of the ratio $E/(1 - \nu^2)$ (sometimes referred to as the indentation modulus), so that two techniques providing two different combinations of the elastic parameters are necessary to determine both parameters. Bamber et al. combined acoustic microscopy and nanoindentation [6] to estimate E and ν . Hurley et al. proposed a method using atomic force microscope measurements obtained with flexural and torsional modes of vibration of the cantilever [7]. This paper describes a more straightforward method using the first two flexural modes of vibration of the cantilever in scanning microdeformation microscopy and a dedicated identification procedure to decouple the elastic parameters. Experimental measurements on an epoxy photoresist (SU8) thin film are carried out to demonstrate the validity of the method.

2 The scanning microdeformation microscope

The scanning microdeformation microscope (SMM) [8,9] is a kind of AC-force contact microscope. The sensor is classically a micromechanical resonator composed of a rectangular silicon beam with a small sharp sapphire tip (curvature radius of several tens of μm) at the end. The cantilever is glued onto a piezoelectric bimorph transducer at the other end. The transducer excites the vibration of the tip-sample system. The tip remains in contact with the sample and vibrates at several kHz with an amplitude in the nanometer range. Amplitude and phase of the vibrating cantilever are measured with a high sensitivity heterodyne interferometer [10] (Fig. 1). This type of microscope is an effective tool to image surfaces and subsurfaces with heterogeneous local elasticity or to characterize local elastic properties, and can be used to characterize polymers [11,12]. The resonant frequencies depend on the static force applied via the contact stiffness. Using a well-suited model [13,14], the first resonant frequency is usually used to estimate the local indentation modulus. Using the same model, it is proposed herein to decouple the contributions of E and ν from the first two resonant frequencies.

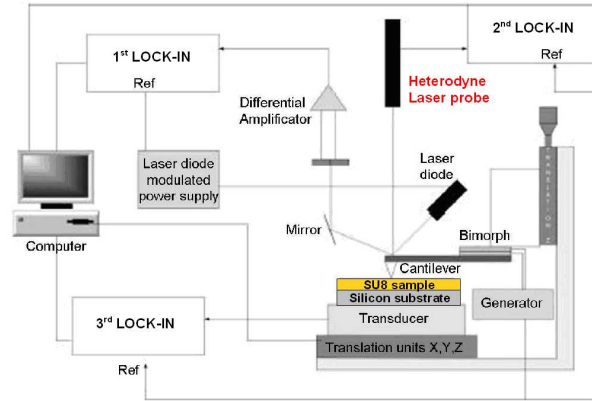


Fig. 1. Schematic view of the SMM setup.

The piezoelectric bimorph transducer action on the cantilever is modeled by a mass-spring system (m_p, K_p) . The interaction with the surface is described by lateral (K_t) and longitudinal (K_n) stiffnesses (Fig. 2). A Hertz contact is considered to relate the contact stiffness to the sample elastic parameters. Assuming the tip's material is much stiffer than the probed material, the lateral and longitudinal stiffnesses are related through $K_t \simeq \frac{2(1-\nu)}{2-\nu} K_n$. K_c denotes the cantilever stiffness.

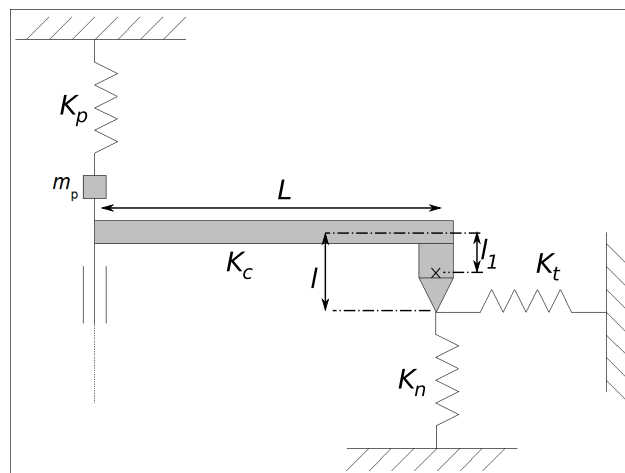


Fig. 2. Model describing the SMM resonator.

3 Materials and Methods

The SU8 resist is a negative epoxy type photoresist which has been developed by IBM (Watson Research Center). This polymer is used for photolithography and MEMS applications and is associated with a low viscoelastic behaviour [15,16]. This resist can now be spin-coated and processed at low thicknesses [17] and used to fabricate mechanical devices [18]. Young's modulus is typically in the range 3-7 GPa and Poisson's ratio near 0.22-0.4 [19,15,20,21] for bulk material and thin films. These mechanical parameters are expected to be very dependent on the processing parameters. The sample considered herein is made of a 20 μm -thick SU8 layer deposited on a silicon substrate.

As previously described, the micromechanical resonator used herein to probe the elastic properties of the sample is made of a silicon cantilever and a sapphire tip with the parameters described in table 1. It should be highlighted these geometrical parameters optimize the frequency sensitivity for materials whose Young's modulus is about few GPa ($K_n \simeq K_c$) [12,16].

The contact resonant frequencies on the SU8 thin layer have

Table 1

Characteristics of the cantilever and the tip.

Length L	Width b	Thickness h	Tip radius R_t
6.5 mm	400 μm	80 μm	45 μm
Tip length l	Tip mass m	Tip's center of mass position l_1	Piezo mass m_p
697 μm	0.44 mg	250 μm	2.3 mg

been recorded (Fig. 3). The applied static force is $F = 0.06$ mN. The first two resonances occur for excitation frequencies equal to 13.7 ± 0.01 kHz (mode 1) and 23.25 ± 0.01 kHz (mode 2).

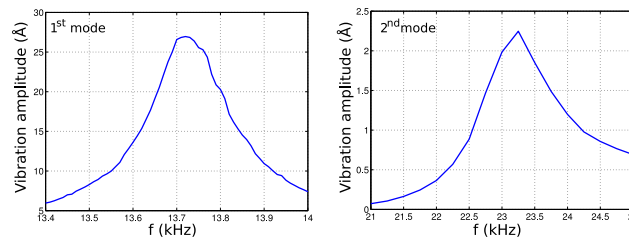


Fig. 3. Amplitude of vibration (Å) as a function of the excitation frequency (kHz) for a static force of 0.06 mN on the 20 micrometers thick SU8 film : first (left) and second mode (right).

4 Identification procedure

4.1 Direct problem

If the elastic properties of the sample are known, the resonant frequencies of the beam are obtained by solving the linear differential equation for the vibration of the beam (*i.e.*, the direct problem)

$$E_c I_n \frac{\partial^4 y}{\partial x^4} + \rho A \frac{\partial^2 y}{\partial t^2} = 0 \quad (1)$$

considering harmonic solutions with the suited boundary conditions. $E_c I_n$ is the cantilever's flexural stiffness, ρ is the cantilever's material mass density. The beam's cross-section is also described through its area $A = bh$. For the system described in Fig.2 the resonance condition is obtained as a closed form ??:

$$0 = R(x, m, AL, l_1) + f(x, m, AL)6l^2Y + 3g(x, m, AL, l_1)X + 18l^2XY \quad (2)$$

where l is the total tip length and l_1 is the distance from the beam's neutral fiber to the tip's center of mass m . R , f and g are non-linear functions. The constitutive parameters appear through the unknowns X and Y

$$X = \frac{K_n}{K_c} \quad (3)$$

$$Y = \frac{K_n}{K_c} \frac{1 - \nu}{2 - \nu} \quad (4)$$

x denotes the frequency parameter defined by

$$x = L \left(\frac{(2\pi f_r)^2 \rho A}{E_c I_n} \right)^{\frac{1}{4}} \quad (5)$$

L is the cantilever's length, f_r is the considered resonant frequency. Eq (2) therefore allows one to compute the resonant frequencies when the geometry and the constitutive parameters are known.

4.2 Inverse problem

Because the first two resonance modes involve different combinations of the lateral and longitudinal stiffnesses, they involve different combinations of the constitutive parameters. To extract the elastic parameters of the sample from the resonant frequencies, one now considers that the resonant frequencies are measured (*i.e.*, known) and that the constitutive parameters are to be retrieved. Considering two different resonance modes, corresponding to the resonance parameters x_1 and x_2 , and discarding the dependences to the geometrical parameters for the sake of

brevity, the parameters satisfy the linear relationship

$$0 = R(x_1) - R(x_2) + (f(x_1) - f(x_2)) 6l^2Y + 3(g(x_1) - g(x_2)) X \quad (6)$$

The vector U is defined by

$$\begin{aligned} U^t &= [g(x_1) - g(x_2), f(x_1) - f(x_2)] \\ &= \|U\| \tilde{U}^t = \|U\| [\tilde{U}_x, \tilde{U}_y] \end{aligned} \quad (7)$$

where U^t is the transpose of U and $\|U\|$ is its norm. Denoting S the sought parameters $S^t = [3X, 6l^2Y]$, the Eq. (6) reads

$$\tilde{U}^t S = \frac{1}{\|U\|} \{R(x_2) - R(x_1)\} = p \quad (8)$$

The solution therefore reads

$$S = (\tilde{U}^t S) \tilde{U} + q\hat{U} \quad (9)$$

with $\hat{U}^t = [\hat{U}_x, \hat{U}_y]$ satisfying

$$\hat{U}^t \hat{U} = 1 \quad (10)$$

$$\hat{U}^t \tilde{U} = 0 \quad (11)$$

U , and consequently \tilde{U} and \hat{U} are obtained from the measured resonant frequencies. p is also known from the resonant frequencies and Eq.(8), so that one only needs to find the scalar q to retrieve the unknown vector S . The Eq.(2) is then recast, for a

given frequency number x

$$\begin{aligned}
0 &= [R(x) + p^2 \tilde{U}_x \tilde{U}_y + p (\tilde{U}_y f(x) + \tilde{U}_x g(x))] \\
&\quad + q [\hat{U}_y f(x) + \hat{U}_x g(x) + p (\tilde{U}_x \hat{U}_y + \tilde{U}_y \hat{U}_x)] + q^2 \hat{U}_x \hat{U}_y \\
&= T(x, q)
\end{aligned} \tag{12}$$

thereby providing a scalar condition per resonance mode depending on q . Assuming Eq.6 is satisfied, only one of the non-linear equations (12) has to be enforced. The initial problem then turns into solving the linear equation (6) and a single non-linear one ($T(x_1, q) = 0$ for instance).

5 Results and discussion

The equation $T(x_1, q) = 0$ is first built using the measured resonant frequencies and solved for q , assuming $K_p = 55 \times 10^3 \text{N.m}^{-1}$ (obtained from the first unloaded resonant frequency) . p is obtained from x_1 and x_2 using Eq.8, so that two solution vectors S are obtained using the two solutions for $T(x_1, q) = 0$. The solution satisfying the linear elasticity theory constrain $\frac{1}{3} \leq \frac{1-\nu}{2-\nu} \leq \frac{2}{3}$ is kept. This provides an initial guess for q which is subsequently polished by minimizing the norm of the vector $J(q)^t = [T(x_1, q), T(x_2, q)]$ with respect to q (Nelder-Mead simplex algorithm). The solution for q is therefore used to build the vector S

thus providing the parameters $X = K_n/K_c = 305.54 \pm 0.4$ and $\nu = 0.38 \pm 0.015$. Using Hertz theory [22], this translates to

$$\frac{E}{1 - \nu^2} = \sqrt{\frac{(XK_c)^3}{6R_tF}} = 7.24 \pm 0.02 \text{ GPa} \quad (13)$$

Considering the values obtained for three samples yields $\frac{E}{1 - \nu^2} = 6.89 \pm 0.58$ GPa. Using nano-indentation tests (continuous stiffness method at 45 Hz), a comparable value ($E/(1 - \nu^2) = 6.42 \pm 0.25$ GPa) has been obtained on the same samples (NanoII nano-indenter from Nano Instruments), thereby proving the identification procedure yields consistent results. The elastic parameters are then decoupled from a single experiment to yield $E = 6.15 \pm 0.07$ GPa and $\nu = 0.38 \pm 0.015$. Again, these values are comparable to previously reported values [19,15,16,20] obtained using different techniques. The obtained value for E is particularly close to the one reported by Al-Halhouli et al.[15]. It should be highlighted the values reported herein are obtained for deformations confined in a volume radiating from the contact point at a distance which scales as $(\frac{3FR_t}{4E})^{\frac{1}{3}} \simeq 690$ nm [22]. The identified constitutive parameters can therefore be considered as local, so that the ability to decouple elastic constants from multiple resonant modes makes this characterization method a powerful

tool for mapping thin-films materials properties. It should be highlighted that even though the described technique applies to isotropic materials, the (qualitative) existence of an anisotropic behavior can be easily tested by changing the cantilever direction (K_t is probed within the plane of Fig.2). The identification technique described herein for isotropic materials and the very promising obtained results therefore pave the way to a quantitative extension to anisotropic materials.

Acknowledgements

The authors gratefully acknowledge S. Keller and M. Knutzen from Nanotech-DTU (Denmark) for providing the SU8 samples.

References

- [1] Lee S.S., Ahn B., Yamanaka K. Characterization of delamination in titanium nitride coating on steel using acoustic microscopy. *J. Mater. Sci.* 1999; 34:6095.
- [2] Capella B., Dietler G. Force-distance curves by atomic force microscopy. *Surf. Sci. Report.* 1999; 34:1.
- [3] Rabe U., Arnold W. Acoustic microscopy by atomic-force microscopy. *Appl. Phys. Lett.* 1994; 64:1493.
- [4] Oliver W.C., Pharr G.M. An improved technique for determining hardness and

elastic-modulus using load and displacement sensing indentation experiments. *J. Mater. Res.* 1992; 7:1564.

- [5] Li X., Bhushan B. A review of nanoindentation continuous stiffness measurement technique and its applications. *Mater. Charact.* 2002; 48:11.
- [6] Bamber M.J., Cooke K.E., Mann A.B., Derby B. Accurate determination of Young's modulus and Poisson's ratio of thin films by a combination of acoustic microscopy and nanoindentation. *Thin Solid Films* 2001; 398:299.
- [7] Hurley D.C., Turner J.A. Measurement of Poisson's ratio with contact-resonance atomic force microscopy. *J. Appl. Phys.* 2007; 102:033509.
- [8] Sthal F., Cretin B. Scanning microdeformation microscopy. *Appl. Phys. Lett.* 1993 ; 62:829.
- [9] Vairac P., Cretin B. Scanning microdeformation microscopy in reflection mode. *Appl. Phys. Lett.* 1996 ; 68:461.
- [10] Vairac P., Cretin B. New structures for heterodyne interferometric probes using double-pass. *Opt. Commun.* 1996; 132:19.
- [11] Arinéro R., Lévêque G., Girard P., Ferrandis J.Y. Image processing for resonance frequency mapping in atomic force modulation microscopy. *Rev. Sci. Instr.* 2007; 78:023703.
- [12] Le Rouzic J., Vairac P., Cretin B., Delobelle P. Sensitivity optimization of the scanning microdeformation microscope and application to mechanical characterization of soft materials. *Rev. Sci. Instr.* 2008; 79:033707.
- [13] Vairac P., Cretin B. Electromechanical resonator in scanning microdeformation microscopy : theory and experiment. *Surf. Interface Anal.* 1999; 27:588591.
- [14] Dupas E., Gremaud G., Kulik A., Loubet J.L. High-frequency mechanical spectroscopy with an atomic force microscope. *Rev. Sci. Instr.* 2001;

72:38913897.

- [15] Al-Halhouli A.T., Kampen I., Krah T., Buttgenbach S. Nanoindentation testing of SU-8 photoresist mechanical properties. *J. Microelectr. Eng.* 2008; 85:942.
- [16] Le Rouzic J., Delobelle P., Vairac P., Cretin B. Comparison of three different scales techniques for the dynamic mechanical characterization of two polymers (PDMS and SU8). *Eur. Phys. J. Appl. Phys.* 2009; 48:11201.
- [17] Keller S., Blagoi G., Lillemose M., Haefliger D., Boisen A. Processing of thin SU8 films. *J. Micromech. Microeng.* 2008; 18:125020.
- [18] Keller S., Haefliger D., Boisen A. Fabrication of thin SU8 cantilevers : initial bending, release and time stability. *J. Micromech. Microeng.* 2010;20:045024.
- [19] Feng R., Farris R. J. The characterization of thermal and elastic constants for an epoxy photoresist SU8 coating. *J. Mater. Sci.* 2002;37:4793.
- [20] Lau G.K., Goosen J.F.L., Van Keulen F., Chu Duc T., Sarro P.M. Powerful polymeric thermal microactuator with embedded silicon microstructure. *Appl. Phys. Lett.* 2007; 90:214103.
- [21] Mcleavey A., Coles G., Edwards R.L., Sharpe Jr. W.N. Mechanical properties of SU-8. *Materials Research Society Symposium - Proceedings* 1999; 546:213.
- [22] H. Hertz, Über die berührung fester elastischer Körper (On the contact of rigid elastic solids) In: *Miscellaneous Papers*; Jones and Schott, London, 1896.